

Single Source Molecular Precursors to Niobia–Silica and Niobium Phosphate Materials[#]

Claus G. Lugmair and T. Don Tilley*

Department of Chemistry, University of California, California 94720-1460, Berkeley
and the Chemical Sciences Division, Lawrence Berkeley National Laboratory,
Berkeley, CA 94720

Received November 3, 2005; accepted (revised) January 13, 2006
Published online March 17, 2006 © Springer-Verlag 2006

Summary. The molecular precursors $\text{Nb}(\text{O}^i\text{Pr})_2[\text{OSi}(\text{O}^t\text{Bu})_3]_3$ and $\{\text{Nb}(\text{O}^i\text{Pr})_4[\text{O}_2\text{P}(\text{O}^t\text{Bu})_2]\}_2$ have been prepared. The first compound undergoes facile thermal conversion to high surface area, acidic niobia silica, whereas the second one thermally decomposes to a low surface area niobium phosphate.

Keywords. Niobia; Siloxide; Phosphate; Molecular precursors; Silicate.

Introduction

Hydrated Nb_2O_5 and Ta_2O_5 exhibit high acid strengths making these oxides useful catalysts for reactions that involve water as a reagent or byproduct, such as esterification, condensation, and hydration reactions [1]. Thermal treatment of these oxides to temperatures above 600°C results in loss of acidity with concomitant dehydration, crystallization of M_2O_5 , and loss of surface area [2]. Thus, numerous investigations have focused on improving the catalytic properties of Nb_2O_5 and Ta_2O_5 . Strategies typically involve dispersing these oxides on supports such as silica [3], or doping them with other oxides in order to prevent sintering and crystallization of the metal oxide [4]. The interaction between two oxides is well known to result in modification of the surface active sites or the generation of new acid sites not found on the pure metal oxides. *Dumesic et al.* have discussed the properties of acid sites generated by supporting metal oxides on silica [5]. Models predicting acid site generation on homogeneously mixed oxides have been proposed by *Kung* [6] and *Tanabe* [1, 7].

* Corresponding author. E-mail: tdtalley@berkeley.edu

[#] Dedicated to Prof. Dr. *Ulrich Schubert*, in honor of his 60th birthday, and in recognition of his many seminal contributions to inorganic chemistry

Niobia–silica mixed oxides have been extensively investigated by *Ko et al.* [3a, 8, 9]. At low pretreatment temperatures (100–200°C) this mixed oxide possesses strong *Brønsted* acidity whereas at higher temperatures (300°C) *Lewis* acidity predominates. Based on *Raman* spectroscopic studies, it was proposed that NbO₄ tetrahedra are the dominant species present after heat treatment to 500°C. The total acidity of the mixed oxide did not decrease until Nb₂O₅ crystallized, indicating that acidity originates from highly dispersed metal oxide units.

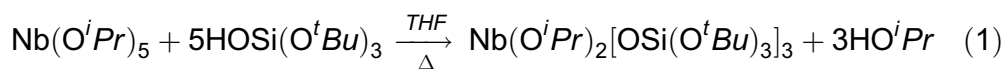
Our approach for the preparation of highly homogeneous mixed element oxide materials entails the use of oxygen rich “single source precursor” complexes containing OSi(*O*^{*t*}Bu)₃ and/or O₂P(*O*^{*t*}Bu)₂ ligands [10]. These types of complexes decompose to form isobutene and water as the primary volatile products leaving carbon-free metal silica or metal phosphate materials. The thermal nature of this transformation allows the synthesis of solid-state materials without the addition of water. Thus, the hydrolysis of *M–O–M'* linkages that are built into the precursors is minimized.

Here we report the synthesis of molecular precursors to Nb₂O₅–SiO₂ and NbPO₅ materials. Solution thermolysis of the niobia–silica precursors produced high surface area xerogels, whereas the niobium phosphate precursor produced a low surface area powder. Some of the physical properties of these solid-state materials are also described.

Results

Synthesis and Characterization of the Precursor Complexes

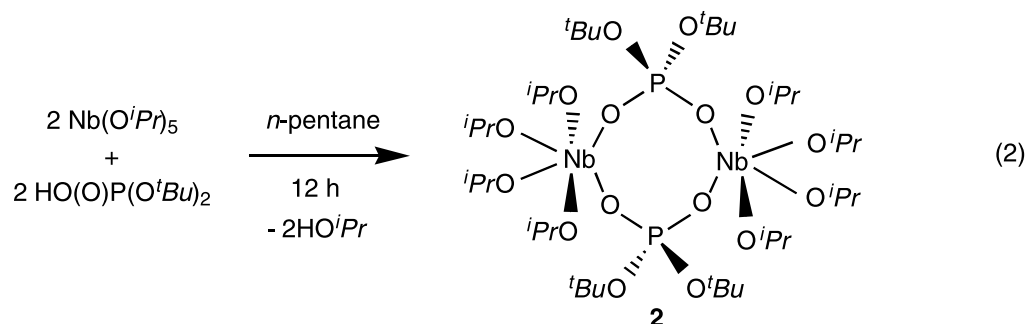
The reaction between Nb(*O*^{*i*}Pr)₅ and excess HOSi(*O*^{*t*}Bu)₃ in refluxing *THF* resulted in elimination of three equivalents of isopropanol and the formation of Nb(*O*^{*i*}Pr)₂[OSi(*O*^{*t*}Bu)₃]₃ (**1**, Eq. (1)).



The use of a stoichiometric amount of HOSi(*O*^{*t*}Bu)₃ (3 equiv.) produced mixtures of the bis- and tris(siloxide) complexes after 24 h at room temperature. The products were isolated by evaporation of the solvent under vacuum and removal of the excess silanol by sublimation at 40°C. Room temperature ¹H and ¹³C NMR spectra for **1** reveal one set of resonances for the alkoxy groups and one resonance for the siloxy ligands.

Addition of a pentane solution of one equivalent of HO₂P(*O*^{*t*}Bu)₂ to a pentane solution of Nb(*O*^{*i*}Pr)₅ produced the niobium phosphate complex {Nb(*O*^{*i*}Pr)₄[O₂P(*O*^{*t*}Bu)₂]}₂ (**2**, Eq. (2)). This highly soluble material was crystallized from CH₂Cl₂ in 76% yield. Room temperature multinuclear NMR spectroscopy (¹H, ¹³C, ³¹P) of **2** indicates that there is one O₂P(*O*^{*t*}Bu)₂ environment. Resonances for two *O*^{*i*}Pr environments with equal integrated intensity are also observed in the ¹H NMR spectrum. This data is consistent with a dimeric structure with bridging di(*tert*-butyl)phosphate groups and an octahedral coordination environment for niobium. The mass spectrum of **2** did not contain a peak corresponding to the parent ion,

however, the fragmentation pattern was consistent with the loss of organic fragments from a dimer.



Thermolytic Behavior of **1** and **2**

The decomposition behavior of compounds **1** and **2** was initially probed by thermal gravimetric analysis (TGA). The TGA trace for **1** (Fig. 1) shows that weight loss begins near 50°C and a more precipitous weight loss occurs around 200°C. At 1000°C a ceramic yield of 27.3% is obtained, which is 4% lower than the expected ceramic yield for $\text{NbO}_{2.5} \cdot 3\text{SiO}_2$ (31.3%). During the thermolysis of a bulk sample of **1**, a viscous oil was obtained at 150°C. Above 200°C the oily decomposition products solidified. The TGA trace for **2** shows that a gradual weight loss begins near room temperature. At about 150°C, the weight loss becomes more rapid resulting in a ceramic yield of 40.0% at 900°C. Near 1000°C there is a small weight loss resulting in a ceramic yield of 38.8% at 1025°C. This is slightly higher than the expected ceramic yield for NbPO_5 of 37.9%.

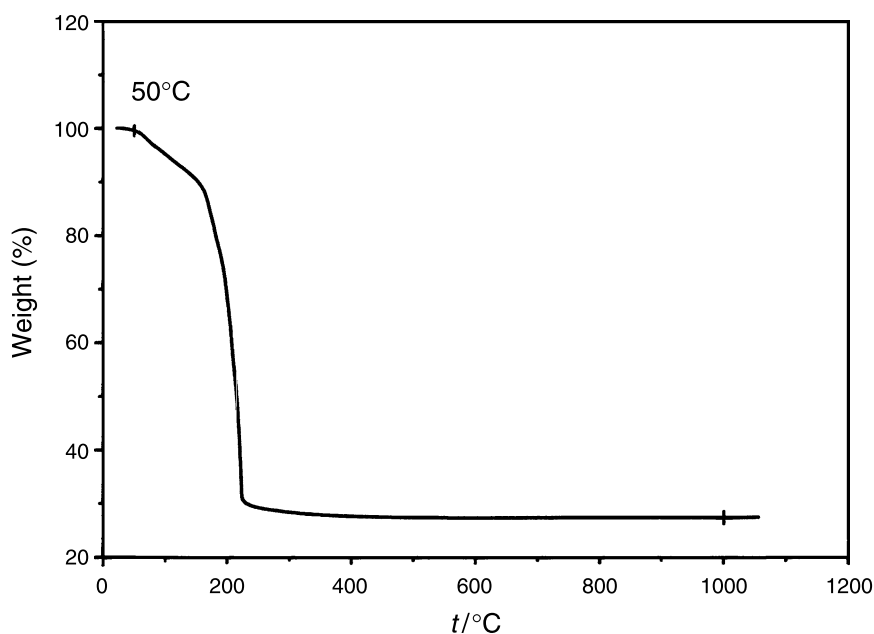


Fig. 1. TGA trace for compound **1** under nitrogen, with a heating rate of 10°C per minute

Solution Phase Thermolyses of **1** and **2**

The facile thermal elimination of organic fragments from **1** and **2** allowed the formation of inorganic networks in solution by thermolytic means. Heating isooctane solutions of **1** to between 145 and 150°C produced soft white gels within 24 h that filled the entire volume the solution originally occupied. Upon air drying, these gels shrank to *ca.* 30% of their original volume and became hard, white materials. Small pieces of these xerogels appeared slightly orange and transparent under magnification. In contrast, an isooctane solution of **2** required heating to 170°C for 9 d in order to form an insoluble material. In this case a very fine white precipitate settled out of solution.

After air drying, these materials were heated to 200°C for 2 h under N₂. Thereafter the materials were calcined at incrementally higher temperatures for 2 h under flowing O₂. After each calcination the samples were analyzed by BET surface area analysis, XRD, and acidity measurements.

Solution thermolysis of **1** and **2** followed by air drying and calcination of the products at 200°C under N₂ resulted in materials with very low organic contents (**1**: C = 1.07%, H = 1.82%; **2**: C = 0.29%, H = 1.20%). Further calcination to 500°C under O₂ lowered the organic content of **1** (C = 0.25%, H = 1.31%).

By elemental analysis, the xerogel derived from **1**, heated to 200°C under N₂, has a Nb:Si ratio of 1:3.06, which is very close to the stoichiometry in the precursor complex (found: Nb = 24.14%, Si = 22.32%). Similarly, the material derived from **2** has a Nb:P ratio of 1:1.02 which is very close to the expected ratio of 1:1 (found: Nb = 39.45%, P = 12.92%). The Nb, Si, and P analyses were lower than expected for pure Nb₂Si₆O₁₇ (calcd: Nb = 29.67%, Si = 26.91%) and NbPO₅ (calcd: Nb = 45.57%, P = 15.19%). This is presumably due to a significant amount of water that is adsorbed on these materials and the small amount of carbon left in the samples.

Although the ceramic yield of the solid state thermolysis of **1** is low due to the volatilization of HOSi(*O*^{*t*}Bu)₃, resulting in silica-poor materials, in solution free silanol is readily decomposed to silica in the presence of niobia- and tantalum-containing gels. Samples of the air-dried gels (4 mg) derived from **1** were added to benzene-*d*₆ solutions of HOSi(*O*^{*t*}Bu) and sealed in an NMR tube. After 12 h at room temperature, 7% of the silanol were consumed with the formation of isobutene and *t*BuOH in a 1:1.6 ratio over the xerogel from **1**. Heating the samples to reflux for 10 min led to a 78% conversion of the silanol giving an isobutene: *t*BuOH ratio of 3.3:1 over the xerogel from **1**.

The xerogel derived from **1** exhibits a very high surface area (490 m² g⁻¹) after calcination to 200°C. Upon calcination above 500°C this sample loses surface area and by 1300°C the surface area is reduced to <5 m² g⁻¹. The precipitate derived from **2** has a very low surface area (<5 m² g⁻¹) even after a mild heat treatment to 200°C. Thermolysis of the xerogel from **1** at 500°C under O₂ yields a material with a surface area of 507 m² g⁻¹ and a total pore volume of 3.0 cm³ g⁻¹. The nitrogen adsorption isotherm is of type IV with a type H1 [11] (formerly type A) [12] hysteresis loop typically found to arise from condensation in cylindrical pores. The average pore diameter is 233 Å and the pore size distribution is very broad including a significant number of pores with a diameter above 1000 Å.

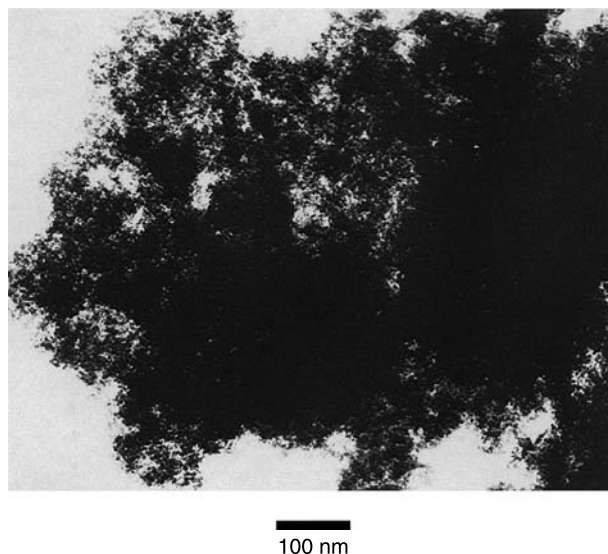


Fig. 2. TEM image of the xerogel derived from **1** after calcination under oxygen at 500°C

Figure 2 shows a TEM micrograph of the xerogel from **1** after calcination to 500°C under O₂. This niobia–silica material consists of fairly well defined spherical grains with diameters between 15 and 25 Å. The xerogel derived from **1** remained amorphous until *ca.* 900°C, where diffraction peaks corresponding to an orthorhombic phase of Nb₂O₅ were first observed. This phase is denoted as the T (tief) modification of Nb₂O₅ in the literature [13]. At this point the average crystalline domain size was about 7 nm as estimated by the *Scherrer* equation [14]. Upon calcination to 1100°C the average crystallite size increased to 12 nm. Calcination to 1300°C resulted in a phase change from T-Nb₂O₅ to M-Nb₂O₅ [13a, 15], a monoclinic modification, with an average crystallite size of 30 nm. At this point a very small diffraction peak corresponding to cristobalite was also detected. The precipitate derived from **2** remained amorphous after calcination to 900°C. After heat treatment to 1100°C diffraction peaks corresponding to t-NbPO₅ (tetragonal phase) [16] with an average particle size of 26 nm and one peak corresponding to m-NbPO₅ (monoclinic phase) [17] were observed. Calcination to 1300°C improved the crystallinity of the monoclinic phase, as determined by the appearance of several additional reflections for this phase, however the particle size remained about the same (as estimated by the *Scherrer* equation).

The acid strength of the xerogel prepared from **1** and the precipitate from **2** were estimated by contacting the solids with toluene or isooctane solutions of various *Hammett* indicators (Table 1) [7b]. The appearance of the acid color of the indicator implied that the solid has acid sites whose *Hammett* acidity function (*H*₀) is equal or less than the *pK*_a value of the indicator. In Table 1 a color change is indicated by a positive sign (+) and the absence of a color change is indicated by a negative sign (–). The xerogel containing Nb oxide has surface acid sites strong enough to protonate benzalacetophenone (*pK*_a = –5.6), but not anthraquinone (*pK*_a = –8.2). These acid sites were retained after calcination to 1100°C. After calcination to 1300°C, this xerogel had no detectable acidity. The precipitate

Table 1. Table showing the surface acid strength of the xerogel from **1** and the precipitate from **4** measured using various *Hammett* indicators; the appearance of the acid color of the indicator is indicated by a + sign and the absence of a color change is indicated by a – sign

Calcination temperature/°C (atmosphere)	pK_a of <i>Hammett</i> indicator				
	+4.8	+1.5	–3.0	–5.6	–8.2
Nb₂O₅–3SiO₂					
200 (N ₂)	+	+	+	+	–
500 (O ₂)	+	+	+	+	–
700 (O ₂)	+	+	+	+	–
900 (O ₂)	+	+	+	+	–
1100 (O ₂)	+	+	+	+	–
1300 (O ₂)	–	–	–	–	–
NbPO₅					
200 (N ₂)	–	–	–	–	–
500 (O ₂)	–	–	–	–	–
700 (O ₂)	+	+	+	–	–
900 (O ₂)	+	+	+	–	–
1100 (O ₂)	+	+	+	–	–
1300 (O ₂)	+	+	+	–	–

derived from **2** had no detectable acidity after calcination to 500°C. After calcination to 700°C the material possessed acid sites that protonated dicinnamalacetone ($pK_a = -3.0$) but not benzalacetophenone ($pK_a = -5.6$). This acidity was retained after calcination to 1300°C for 2 h.

Discussion

The niobium siloxide precursor **1** is readily prepared by alcohol elimination from corresponding pentaalkoxides. Complexes containing more than three siloxide ligands were obtained even under forcing conditions. Similarly, *Wolczanski* has reported Nb and Ta complexes containing never more than three tritox (tBu_3CO) or silox (tBu_3SiO) ligands [18]. In contrast, *Bradley* has reported the homoleptic siloxide, Ta(OSiMe₃)₅, containing the less sterically demanding OSiMe₃ ligand [19]. Presumably, the structure of **1** is similar to that of the related tantalum complex Ta(OEt)₂[OSi(O^{*t*}Bu)₃]₃, which is monomeric and contains a chelating OSi(O^{*t*}Bu)₃ ligand [20].

The thermolysis behavior of **1** is markedly different from what is observed for the group 4 metal tetrasiloxides, M[OSi(O^{*t*}Bu)₃]₄ (M = Zr, Hf). The Zr and Hf siloxides display a very abrupt weight loss with the formation of 12 equivalents of isobutene and 6 equivalents of water and a theoretical ceramic yield for MSi₄O₁₀. Thermolysis of the Nb complex, on the other hand, produces large quantities of alcohols as well as HOSi(O^{*t*}Bu)₃, resulting in ceramic yields lower than expected for M₂O₅·6SiO₂.

Complex **1** is a good precursor for the thermal preparation of homogeneous mixed oxide gels in organic solvents. The metal-to-silicon ratios in the xerogel pre-

pared from **1** are very similar to the ratio found in the precursors (1M:3Si). Any free $\text{HOSi}(O^tBu)_3$ that is formed during the thermolysis is rapidly decomposed to silica, isobutene, and water. The xerogel prepared in toluene has a high surface area ($507 \text{ m}^2 \text{ g}^{-1}$), even after calcination to 500°C . *Ko et al.* prepared a Nb_2O_5 – SiO_2 xerogel [3a] and an aerogel [9b], each having a Nb:Si ratio of 1:7. After calcination to 500°C these materials had surface areas of $480 \text{ m}^2 \text{ g}^{-1}$ and $670 \text{ m}^2 \text{ g}^{-1}$. The higher surface area of these materials may be partially attributed to their higher silica content.

As with other multicomponent mixed oxide ceramics the temperature at which a single component metal oxide phase separates and crystallizes can be used as a gauge of the original homogeneity of the mixed material [9b]. For well-mixed oxides more extensive diffusion must occur prior to nucleation and grain growth. This will delay the appearance of crystalline single component oxides. Bulk Nb_2O_5 can exist in several crystalline modifications, the most common of which are denoted by the letters T (tief), M (medium), and H (high) [13a]. Amorphous Nb_2O_5 crystallizes into the T phase at *ca.* 500°C , into the M phase at *ca.* 800°C , and into the H phase at *ca.* 1000°C [21]. The effect of the silica phase on the crystallization behavior of Nb_2O_5 is evident in the thermolysis behavior of the xerogel derived from **1**. For this material, crystallization of the T phase is delayed until 900°C and transformation to the M phase is not observed until 1300°C . Similarly, the Nb_2O_5 – SiO_2 materials prepared by *Ko* remained amorphous up to 800°C and by 1000°C a low temperature phase of Nb_2O_5 had crystallized [3a, 9].

The strength of the strongest acid sites on Nb_2O_5 – SiO_2 were estimated using several *Hammett* indicators. The results indicate that strong acid sites ($pK_a \leq -5.6$) are present on the surface even after calcination to 1100°C . At these temperatures poorly crystalline M_2O_5 is present in the materials (by XRD). However, a significant portion of the metal oxide must remain finely dispersed in the silica since bulk Nb_2O_5 is known to have negligible acidity after calcination to 500°C [2]. The further phase separation and crystal growth of the Nb_2O_5 phases at 1300°C renders these materials nonacidic. At this temperature the material also becomes nonporous.

Unfortunately, the thermolytic decomposition of **2** in toluene only produces low surface area precipitates. The precipitate remains amorphous to very high temperatures (1100°C), at which point t-NbPO₅ and small amounts of m-NbPO₅ crystallize. Monoclinic NbPO₅ is known to form by thermolysis of $\text{Nb}_2\text{O}_5 \cdot 2\text{P}_2\text{O}_5$ at 1070°C with the loss of volatile P_2O_5 [22]. The small weight loss observed in the TGA curve for the precipitate derived from **2** at *ca.* 1000°C suggests that m-NbPO₅ crystallizes from phosphorous rich regions of the sample in a similar manner. Amorphous niobium phosphate, prepared from potassium niobate and phosphoric acid, crystallizes at *ca.* 830°C to NbPO₅ [4b]. The late crystallization of the precipitate derived from **2** and the formation of m-NbPO₅ indicate that the precipitate is not very homogeneous. Interestingly this precipitate is not acidic when calcined to 200°C or 500°C but has moderately strong acid sites when calcined between 700 and 1300°C . Studies of other niobium phosphate materials show that strong acidity is obtained at low pretreatment temperatures and that acid strength as well as the number of acid sites decreases with calcination temperature [4a, b].

Conclusions

New single source molecular precursors were obtained for the preparation of Nb₂O₅–SiO₂ and NbPO₅ materials. High surface area Nb₂O₅–3SiO₂ xerogels can be readily prepared in organic solvents *via* mild thermolysis. The highly homogeneous nature of these xerogels is reflected in the late crystallization of the phase-separated metal oxides. Unlike the homoleptic Zr and Hf siloxide precursors, the Nb mixed ligand siloxide precursor decomposes in the solid state to form significant amounts of silanol. The reason for this behavior is yet unclear. Strong acid sites are retained in these materials to surprisingly high calcination temperatures.

Experimental

All manipulations were performed under a nitrogen atmosphere using standard *Schlenk* techniques or a Vacuum Atmospheres dry box. Diethyl ether, *THF*, and *n*-pentane were distilled from Na benzophenone under N₂. Toluene and benzene were distilled from Na under N₂ and then degassed. NMR spectra were recorded on a Bruker AMX-300 spectrometer at 300 (¹H), 75.5 (¹³C), or 121.5 (³¹P) MHz, or on a Bruker AMX-400 spectrometer at 400 (¹H), 100 (¹³C), or 161 (³¹P) MHz. Benzene-*d*₆, vacuum transferred from a Na/K alloy, was used as the solvent for all NMR studies. Infrared spectra were collected as Nujol mulls on a Mattson galaxy 3000 spectrometer, using CsI cells. Thermolyses were performed using a *Lindberg* 1700°C or a *Lindberg* 1200°C three zone tube furnace. Heat treatments were carried out under flowing (500 cm³ min⁻¹) N₂ (99.98%) or O₂ (99.96%). Electron microscopy was performed on a JEOL 100CX. Thermal analyses were performed on a DuPont model 2000 thermal analysis system. Powder X-ray diffraction was performed on a Siemens D5000 spectrometer. Volatile thermolysis products were separated using a Hewlett Packard HP5890 gas chromatograph with a 30M-DB5MS column and a 5970A series mass selective detector. The compounds HO₂P(*O*^{*i*}Bu)₂ [23], HOSi(*O*^{*i*}Bu)₃ [24], and Nb(*O*^{*i*}Pr)₅ [25] were prepared according to published procedures.

Nb(*O*^{*i*}Pr)₂[*OSi*(*O*^{*i*}Bu)₃]₃ (**1**)

A *THF* solution (25 cm³) of HOSi(*O*^{*i*}Bu)₃ (3.40 g, 12.9 mmol) was added dropwise to a *THF* solution (25 cm³) of 1.00 g Nb(*O*^{*i*}Pr)₅ (2.58 mmol). The reaction mixture was heated to reflux for 5 h. The solvent was then removed *in vacuo*, and the excess HOSi(*O*^{*i*}Bu)₃ was sublimed from the product at 70°C/0.001 mm Hg over 4 h. The remaining white solid was extracted into 20 cm³ pentane. The solution was filtered, concentrated to 5 cm³, and cooled (–40°C) to afford 1.44 g **1** as colorless crystals in 56% yield. Anal: calcd. for C₄₂H₉₅O₁₄Si₃Nb C 50.37 H 9.56, found C 50.04 H 9.68; ¹H NMR (400 MHz): δ = 5.44 (sept, 2H, *J* = 6.1 Hz, OCH(CH₃)₂), 1.51 (s, 81H, OSi(*O*^{*i*}Bu)₃), 1.47 (d, 12H, *J* = 6.1 Hz, OCH(CH₃)₂) ppm; ¹³C{¹H} NMR (100 MHz): δ = 76.95 (OCH(CH₃)₂), 72.81 (OC(CH₃)₃), 31.98 (OC(CH₃)₃), 26.41 (OCH(CH₃)₂) ppm; IR (CsI, Nujol): $\bar{\nu}$ = 1387 m, 1364 m, 1241 m, 1215 w sh, 1192 m, 1127 m, 1067 s, 1056 s, 1028 msh, 980 m, 923 s, 851 w, 831 w, 701 m, 658 vw, 591 m, 547 vw, 513 w sh, 494 w, 470 m, 430 w sh cm⁻¹.

[*i*PrO)₄Nb(O₂P(*O*^{*i*}Bu)₂)]₂ (**2**)

A pentane solution (20 cm³) of HO₂P(*O*^{*i*}Bu)₂ (0.50 g, 2.38 mmol) was added dropwise to a stirring *n*-pentane solution (20 cm³) of Nb(*O*^{*i*}Pr)₅ (0.924 g, 2.38 mmol). The reaction mixture was allowed to stir for 12 h. The solvent was then removed *in vacuo*, and the remaining white solid was extracted into 20 cm³ CH₂Cl₂. The solution was filtered, concentrated to 5 cm³, and cooled (–80°C) to afford 0.975 g of **2** as colorless crystals in 76% yield. Anal: calcd. for C₂₀H₄₆NbO₈P C 44.68 H 8.62, found C 44.50 H 8.85; MS (EI, 70 eV): *m/e* (%) (M = dimer) = 1017 (80) [M⁺ – *O*^{*i*}Pr], 958 (60) [M⁺ – 2*O*^{*i*}Pr], 915 (60) [M⁺ – *O*^{*i*}Pr – HO^{*i*}Pr – H₂C=CHCH₃], 901 (20) [M⁺ – *O*^{*i*}Pr – HO^{*i*}Pr – H₂C=CHCH₃]; ¹H NMR (400 MHz): δ = 5.08 (sept, 2H, *J* = 6.1 Hz, NbOCH(CH₃)₂), 4.97 (sept, 2H, *J* = 6.1 Hz,

$\text{NbOCH}(\text{CH}_3)_2$, 1.57 (s, 18H, $\text{O}_2\text{P}(\text{O}^i\text{Bu})_2$), 1.49 (d, 12H, $J = 6.1$ Hz, $\text{NbOCH}(\text{CH}_3)_2$), 1.41 (d, 12H, $J = 6.1$ Hz, $\text{NbOCH}(\text{CH}_3)_2$) ppm; $^{13}\text{C}\{^1\text{H}\}$ NMR (100 MHz): $\delta = 79.86$ (d, $^2J_{\text{CP}} = 8$ Hz, $\text{OC}(\text{CH}_3)_3$), 77.20 (s, $\text{OCH}(\text{CH}_3)_2$), 73.72 (s, $\text{OCH}(\text{CH}_3)_2$), 30.46 (d, $^3J_{\text{CP}} = 4$ Hz, $\text{OC}(\text{CH}_3)_3$), 26.34 (s, $\text{OCH}(\text{CH}_3)_2$), 25.61 (s, $\text{OCH}(\text{CH}_3)_2$) ppm; $^{31}\text{P}\{\text{H}\}$ NMR (161.9 MHz): $\delta = -20.46$ (s) ppm; IR (CsI, Nujol): $\bar{\nu} = 1601$ m, 1391 m, 1370 m, 1360 w sh, 1325 m, 1253 m sh, 1235 s, 1163 m sh, 1141 s, 1117 m sh, 1084 s, 1038 m sh, 1018 s, 986 s, 919 w, 847 m, 722 w, 697 w sh, 580 s, 491 m sh, 461 m, 443 w sh, 434 vw sh, 412 vw cm^{-1} .

Acknowledgements

This work was supported by the Director, Office of Energy Research, Office of Basic Energy Sciences, Chemical Sciences Division, of the U.S. Department of Energy under contract DE-AC02-05CH11231.

References

- [1] Tanabe K, Misono M, Ono Y, Hattori H (1989) In: Delmon B, Yates JT (eds) *New Solid Acids and Bases: their Catalytic Properties; Studies in Surface Science and Catalysis*, vol 51. Elsevier, New York
- [2] Chen Z, Izuka T, Tanabe K (1984) *Chem Lett* **13**: 1085
- [3] a) Burke PA, Ko EI (1991) *J Catal* **129**: 38; b) Jehng J, Wachs IE (1990) *Catal Today* **8**: 37; c) Nishimura M, Asakura K, Iwasawa Y (1986) *J Chem Soc Chem Commun*: 1660; d) Ichikuni N, Asakura K, Iwasawa Y (1991) *J Chem Soc Chem Commun*: 112; e) Yoshida H, Tanaka T, Yoshida T, Funabiki T, Yoshida S (1996) *Catal Today* **28**: 79; f) Yoshida S, Nishimura Y, Tanaka T, Kanai H, Funabiki T (1990) *Catal Today* **8**: 6; g) Shirai M, Ichikuni N, Asakura K, Iwasawa Y (1990) *Catal Today* **8**: 57; h) Tanaka T, Nojima H, Yoshida H, Nakagawa H, Funabiki T, Yoshida S (1993) *Catal Today* **16**: 297; i) Asakura K, Iwasawa Y (1991) *J Phys Chem* **95**: 1711; j) Tanaka T, Takenaka S, Funabiki T, Yoshida S (1994) *Chem Lett* **23**: 809
- [4] a) Florentino A, Cartraud P, Magnoux P, Guisnet M (1992) *Appl Catal A: General* **89**: 143; b) Okazaki S, Wada N (1993) *Catal Today* **16**: 349; c) Waghay A, Ko EI (1996) *Catal Today* **28**: 41; d) Morikawa A, Ebitani K, Hirano Y (1996) *Catal Today* **28**: 91; e) Mastuura I, Ishimura T, Hayakawa S, Kimura N (1996) *Catal Today* **28**: 133
- [5] a) Connell G, Dumesic JA (1987) *J Catal* **05**: 285; b) Kataoka T, Dumesic JA (1988) *J Catal* **112**: 66
- [6] Kung HH (1984) *J Solid State Chem* **52**: 191
- [7] a) Tanabe K, Sumiyoshi T, Shibata K, Kiyoura T, Kitagawa J (1974) *Bull Chem Soc Jpn* **47**: 1064; b) Tanabe K (1981) In: Anderson JR, Boudart M (eds) *Catalysis Science and Technology*, vol 2. Academic Press, New York, p 231
- [8] DeCanio EC, Nero VP, Ko EI (1994) *J Catal* **146**: 317
- [9] a) Maurer SM, Ko EI (1993) *Catal Today* **16**: 319; b) Maurer SM, Ko EI (1992) *Catal Today* **12**: 231
- [10] a) Tilley TD (2002) *J Molec Catal A Chem* **182–183**: 17; b) Furdala KL, Tilley TD (2003) *J Catal* **216**: 265; c) Cowley AH, Jones RA (1989) *Angew Chem Int Ed Engl* **28**: 1208; d) Veith M (2002) *J Chem Soc Dalton Trans* 2405; e) Murugavel R, Walawalkar MG, Dan M, Roesky HW, Rao CNR (2004) *Acc Chem Res* **37**: 763
- [11] Sing KSW, Everett DH, Haul RAW, Moscou L, Pierotti RA, Rouquerol J, Siemieniowska T (1985) *Pure Appl Chem* **57**: 603
- [12] a) Lowell S, Shields JE (1984) *Powder Surface Area and Porosity*. Chapman and Hall, New York; b) In: Lecloux AJ, Anderson RJ, Boudart M (eds) *Catalysis Science and Technology*. Springer, New York, p 171

- [13] a) Schafer H, Gruehn R, Schulte F (1966) *Angew Chem Int Ed Engl* **5**: 40; b) International Center for Diffraction Data “PC-PDF” vol 2, 1988; Card # 30-873
- [14] Scherrer P (1918) *Nachr Ges Wiss Göttingen*: 96
- [15] International Center for Diffraction Data “PC-PDF” vol 2, 1988; Card # 30-872
- [16] International Center for Diffraction Data “PC-PDF” vol 2, 1988; Card # 19-866
- [17] International Center for Diffraction Data “PC-PDF” vol 2, 1988; Card # 27-1316
- [18] Wolczanski PT (1995) *Polyhedron* **14**: 3335
- [19] Bradley DC, Thomas IM (1959) *J Chem Soc* 3404
- [20] Brutchey RL, Lugmair CG, Schebaum LO, Tilley TD (2005) *J Catal* **229**: 72
- [21] Ko EI, Weissman JG (1990) *Catal Today* **8**: 27
- [22] Levin EM, Roth RS (1970) *J Solid State Chem* **2**: 250
- [23] Goldwhite H, Saunders BC (1957) *J Chem Soc* 2409
- [24] Zwierzak A, Kluba M (1971) *Tetrahedron* **27**: 3163
- [25] Terry KW PhD Thesis, University of California, San Diego, 1993